



The role of local features in shape discrimination of contour- and surface-defined radial frequency patterns at low contrast

Iliya V. Ivanov*, Kathy T. Mullen

McGill Vision Research, Department of Ophthalmology, McGill University, 687 Pine Avenue West, H4-14, Montréal, Canada H3A 1A1

ARTICLE INFO

Article history:

Received 18 May 2011

Received in revised form 1 September 2011

Available online 20 October 2011

Keywords:

Shape discrimination

Contrast

Radial frequency

Curvature

Orientation

Local

Global

ABSTRACT

Shape processing involves a progression from local to global analysis. A key aspect of this is the binding of distributed local features into an overall form followed by the extraction of the shape independently of its local contrast and spatial scales, so enabling the shape to be encoded based on its proportions without reference to its exact size or retinal location. Here we use contour- and surface-defined radial frequency (RF) patterns in a shape discrimination task, previously thought to reflect a global processing stage that has reached contrast and scale invariance. We compare performance across different spatial scales for a wide range of RF patterns (contour spatial frequencies of 0.7–10.0 cpd, pattern radii of 0.5–10.5°), and sharp- and smooth-edged surface-RF patterns, all at low contrast (5× detection threshold). We show that shape discrimination thresholds for RF patterns have a complex series of dependencies on stimulus size (radius), contour spatial frequency (thickness) and contrast, with no scale invariance. Our results are at odds with earlier work showing no effect of radius and spatial frequency on discrimination thresholds. We show that this discrepancy can be accounted for by a differential effect of contrast on shape discrimination, with shape invariance only stabilizing at higher contrasts (10–20× threshold).

© 2011 Elsevier Ltd. All rights reserved.

1. Introduction

Shape processing involves a hierarchical progression from a local to global analysis. A key aspect of this progression is the binding of spatially distributed local features into an overall form, followed by the extraction of the shape independently of its local contrast and spatial scales, so enabling the shape to be encoded based on its proportions without reference to its exact size or retinal location. The physiological origins of these different shape processing stages begin in V1 and V2 where local orientation (Hubel & Wiesel, 1968) and curvature (Dobbins, Zucker, & Cynader, 1987, 1989) are extracted. These local properties are further processed in V4, where concentric and curvature based neural responses have been found (Dumoulin & Hess, 2007; Gallant, Braun, & Van Essen, 1993; Gallant, Shoup, & Mazer, 2000; Pasupathy, 2006; Pasupathy & Connor, 1999, 2001, 2002; Wilkinson et al., 2000). Finally, higher areas, such as the inferotemporal cortex (IT) and the lateral occipital complex (LOC), contain neurons specialized in detection and recognition of whole objects invariant to position and spatial scale (Fujita et al., 1992; Gross, Rocha-Miranda, & Bender, 1972; Ito et al., 1995; Logothetis, Pauls, & Poggio, 1995; Reddy & Kanwisher, 2006).

A stimulus that has been extensively used in the psychophysical investigation of shape perception tasks is the RF pattern (Wilkinson,

Wilson, & Habak, 1998; Wilson & Wilkinson, 1997). This is a radially modulated circular contour, spatially defined by a fourth derivative of Gaussian, that represents outlines of simple symmetrical shapes such as ellipses, triangles and squares (Fig. 1A). Modifications of such patterns have been used in psychophysical studies to investigate the roles of local and global cues in limiting shape discrimination at threshold, in which radial modulation thresholds are measured for the discrimination of the RF pattern from a perfect circle (Bell et al., 2007; Hess, Wang, & Dakin, 1999; Jeffrey, Wang, & Birch, 2002; Loffler, 2008; Loffler, Wilson, & Wilkinson, 2003; Mullen & Beaudot, 2002; Mullen, Beaudot, & Ivanov, 2011; Poirier & Wilson, 2007; Wang & Hess, 2005; Wilkinson, Wilson, & Habak, 1998; Wilson, 1999). Discrimination of these RF patterns at threshold is thought to activate the entire shape-processing pathway from the early local to the higher global stages of global processing (Hess et al., 1999; Jeffrey, Wang, & Birch, 2002; Loffler, 2008; Loffler, Wilson, & Wilkinson, 2003; Poirier & Wilson, 2007; Wang & Hess, 2005; Wilkinson, Wilson, & Habak, 1998; Wilson, 1999), although the involvement of the global stages at threshold has recently been questioned (Mullen, Beaudot, & Ivanov, 2011).

In their seminal paper on RF patterns, Wilkinson, Wilson, and Habak (1998) found that shape discrimination thresholds for RF patterns are invariant to manipulations of local shape features, including the spatial frequency of the contour, the pattern radius, and the contrast. They concluded that RF shape discrimination reflects the operation of a global processing stage that has achieved

* Corresponding author. Fax: +1 514 843 1691.

E-mail address: iliya.ivanov@mcgill.ca (I.V. Ivanov).

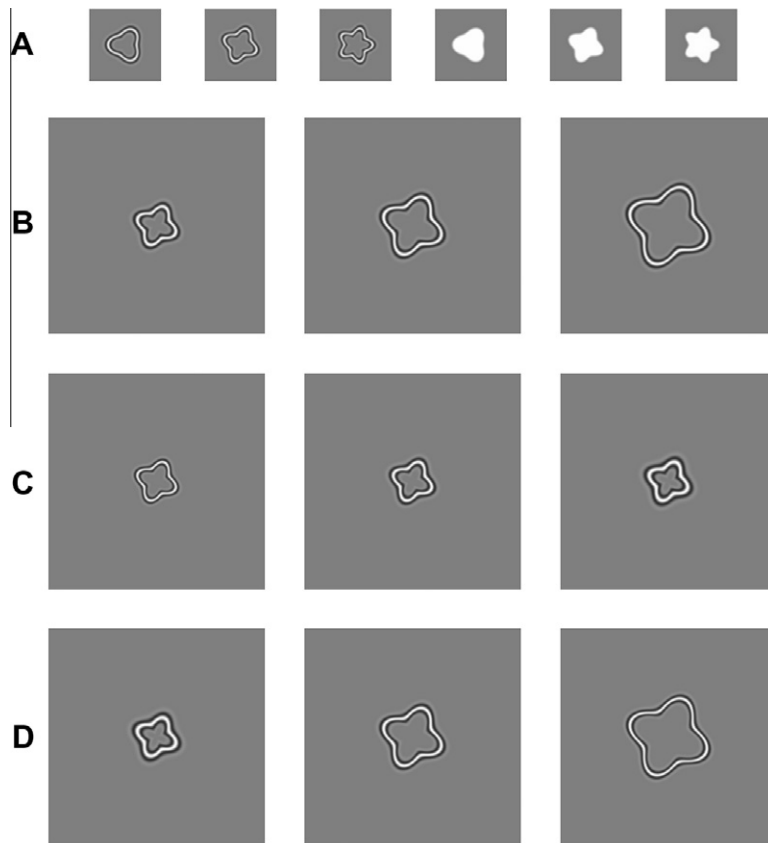


Fig. 1. Row (A) gives an examples of the contour- and surface-defined RF patterns used in our experiments. Row (B) represents examples of the size (radius) change of contour-RF patterns, with the spatial frequency constant. In Row (C), the reverse condition is shown, in which spatial frequency varies and radius is constant. Row (D) illustrates a condition in which viewing distance is varied and the relationship between spatial frequency and size varies inversely. The icons are for illustration only.

shape and contrast constancy and so extracts shape independently of its local properties. Subsequently, however, other studies exploring a different range of stimulus parameters observed that varying the spatial frequency of the contour or overall radius of the shape influenced shape discrimination thresholds (Mullen & Beaudot, 2002; Mullen, Beaudot, & Ivanov, 2011), arguing against shape constancy. All studies, however, have found some evidence for distance scaling with shape discrimination thresholds for particular RF patterns shown to be invariant to a change in viewing distance (Mullen & Beaudot, 2002; Mullen, Beaudot, & Ivanov, 2011; Wilkinson, Wilson, & Habak, 1998). Using gabor-based patterns to study global structure rather than RF patterns, Achtman, Hess, and Wang (2003) demonstrated that mechanisms responsible for detecting the global shape are broadly tuned to a range of local shape features, including the carrier spatial frequency and contrast of the elements, supporting the argument that detecting shape structure can be based on a global processing analysis at threshold that is independent of local features. A further important aspect of shape processing is contrast invariance. Some studies have concluded that the mechanisms responsible for global shape detection are contrast invariant for both gabor-based (Achtman, Hess, & Wang, 2003) and RF patterns (Wilkinson, Wilson, & Habak, 1998). On the other hand, Mullen and Beaudot (2002) using RF patterns found that shape discrimination thresholds are influenced by the contrast, with increasing contrast leading to a monotonic improvement in shape discrimination.

Most previous studies of RF patterns have used high stimulus contrasts, typically 80–100% (Hess et al., 1999; Jeffrey, Wang, & Birch, 2002; Loffler, 2008; Loffler, Wilson, & Wilkinson, 2003; Poirier & Wilson, 2007; Wang & Hess, 2005; Wilkinson, Wilson,

& Habak, 1998; Wilson, 1999). Previous studies that have investigated the effect of stimulus contrast suggest that RF pattern discrimination threshold is invariant with stimulus contrast above a certain level (>10% in Wilkinson, Wilson, and Habak (1998); >20% in Hess et al. (1999); 50% or higher for elderly subjects in Wang et al. (2002)). For this reason, RF pattern discrimination is considered a “supra-threshold” task. The results obtained from these studies favor the involvement of a global pooling mechanism in RF pattern discrimination. Although it is known that the performance of RF pattern discrimination is affected when stimulus contrast is below a certain level, much less is known about how the visual system handles RF pattern processing when the stimulus contrast is low, and below 10% or close to contrast detection threshold. Mullen, Beaudot, and Ivanov (2011) investigated the RF pattern discrimination at low stimulus contrasts, and their results clearly indicated that when stimulus contrast was at $5\times$ contrast detection threshold, the task of discriminating RF patterns no longer involved global pooling. They also showed that the radial modulation thresholds were around 1% (Figs. 2 and 3 in Mullen, Beaudot, and Ivanov (2011)), higher than the typical 0.3–0.4% found in previous studies using higher stimulus contrasts. This suggests that RF pattern discrimination may not be processed by a fully-functioning global pooling mechanism at low contrast levels and other non-global mechanisms mediate shape processing. We therefore expect that non-global mechanisms are likely to determine shape discrimination thresholds at low contrasts.

In this paper, we aim to resolve the controversy over whether the shape discrimination of RF patterns is invariant with the local cue changes of pattern radius and contour spatial frequency, taking into account the effect of contrast. Evidence that shape discrimination

thresholds are independent of the exact composition of the shape's local elements favors the idea that performance is limited at a higher, global processing stage. Alternatively, a lack of shape constancy indicates the importance of local cues in shape processing and suggests that global coding has not been fully achieved. First, we investigate the effect of contour spatial frequency and pattern size (radius) of RF stimuli on shape discrimination thresholds over a range of spatial frequencies (1–10 cpd) and radii (0.5–10°). This is done for an extensive range of different shapes (radial frequencies from 2 to 6 cycles/circ). Second, we explore the effect of contrast scaled at 5–125× detection threshold (3–100% contrast) on shape discrimination thresholds. We scale RF patterns in multiples of their detection thresholds to control for the differences in contrast sensitivity across spatial frequency and retinal location. As well as investigating contrast constancy, this experiment provides an explanation for why previous results have differed. Last, we use a new variation of the RF pattern to investigate whether shape discrimination thresholds are invariant with local edge cues. These patterns have a surface luminance different from the background (called surface-RF) and we investigate the effect of the pattern edge on shape discrimination thresholds (sharp, high spatial frequency vs. smooth, low spatial frequency edges). Similar stimuli have been used in neurophysiological studies of shape processing in primates (Pasupathy, 2006; Pasupathy & Connor, 1999, 2002) and activate single neurons in area V4, representing an intermediate stage in shape processing, which is thought to be global (Pasupathy, 2006).

Overall, for shape discrimination thresholds, we find no evidence for shape constancy across contour spatial frequency, pattern radius or contrast for the contour- and surface-defined RF patterns. Instead, we find evidence for a weaker form of constancy in terms of distance scaling in which the effect of spatial frequency and radius on threshold vary inversely, so maintaining constant threshold across different viewing distances. These findings demonstrate that the highest stage of global processing, shape invariance, is not established for shape discrimination threshold at low contrasts, and point to the importance of local cues for threshold discriminations of RF patterns.

2. Methods

2.1. Stimuli

The stimuli used were achromatic RF and surface-RF patterns. The RF patterns were radially modulated D4s (fourth derivative of a Gaussian) (Wilkinson, Wilson, & Habak, 1998; Wilson & Wilkinson, 1997), with peak spatial frequencies of 1–10 cpd, whose contrasts were equated in multiples of detection threshold. These radial frequency patterns are band-limited in spatial frequency domain, and defined by the equations:

$$RF(r) = L_m[1 + c(1 - 4r^2 + 4r^4/3)e^{-r^2}] \quad (1)$$

$$r(x, y) = \frac{\sqrt{x^2 + y^2} - R(x, y)}{\sigma} \quad (2)$$

$$R(x, y) = R_m\{1 + A \sin[f_r \arctan(y/x) + \theta]\} \quad (3)$$

$$\sigma = \frac{\sqrt{2}}{\pi\omega_p} \quad (4)$$

where σ is the space constant of $RF(r)$ in degrees, ω_p is the D4 peak spatial frequency, $R(x, y)$ is the sinusoidal radial modulation of D4s, R_m is the mean radius, f_r is the radial frequency, A is the amplitude of the radial modulation, and θ is the phase of the modulation (randomly selected in each trial of the experiments). L_m and c are the

mean luminance and contrast, respectively. Circular patterns have no radial modulation ($A = 0$, and thus R is constant).

The surface-RF patterns were created by applying a clipping function on the luminance profile of the RF patterns, such as:

$$L_m(r) = \begin{cases} 1 & L_m(r) > 1 \\ 0 & L_m(r) < 0 \end{cases} \quad (5)$$

where the cut off of the low spatial frequency was 1 cpd.

2.2. Apparatus and calibrations

Stimuli were displayed on a Mitsubishi Diamond Pro monitor (2070 SB) driven by a VSG 2/5 graphics board (Cambridge Research Systems) with 15 bits of contrast resolution, housed in a Pentium PC computer. The frame rate of the display was 120 Hz. The spectral emissions of the red, green and blue guns of the monitor were calibrated using a PhotoResearch PR-650-PC SpectraScan spectroradiometer. The monitor was gamma corrected in software with lookup tables using luminance measurements obtained from an OptiCAL gamma correction system interface with the VSG display calibration software (Cambridge Research Systems). The Smith and Pokorny fundamentals were used for the spectral absorption of the L, M, and S cones. From these data, a linear transform was calculated to specify the phosphor contrasts required for given cone contrasts. The monitor was viewed in a blacked out room. The mean luminance of the display was 60 cd/m². The stimuli were viewed at 60 cm, and the viewing area had size of 1024 × 768 pixels (12.8° × 9.6°). Stimuli were generated on-line, and a new stimulus was generated for each presentation.

2.3. Protocol

In our experiments, cone contrast is expressed in multiples of detection threshold to eliminate the differences in the contrast sensitivity as a function of the spatial frequency of the contour. This allows our stimuli to be matched in terms of suprathreshold contrast units (i.e. matched in visibility). For this scaling, contrast detection thresholds were obtained using a two interval forced choice (2IFC) staircase method for each type of stimulus used: the contour-RF patterns at each combination of spatial frequency and radii that we investigated, and the surface-RF patterns with the different edge spatial frequencies. Unless otherwise given, stimulus contrast was set to 5× detection threshold.

Shape discrimination thresholds were measured using a 2IFC staircase procedure in which radial amplitude modulation was varied. The subject was asked to discriminate between a modulated and non-modulated stimulus (a circle), for contour- and surface-RF patterns and indicate which interval contained the modulated stimulus. In all of our 2IFC staircase procedures, modulation (contrast or shape) was reduced after two correct responses, and increased after one wrong response, corresponding to a criterion of 71% correct responses (2 down, 1 up staircase). The change was 50% before the first reversal, and 25% after the first reversal. Each session was terminated after six reversals, and the detection threshold was computed from the mean of the last five reversals. All plotted data points show the mean and standard error of at least 3 threshold measurements. In all procedures, the exact location of the stimulus was varied randomly from trial to trial about the display centre by adding a positional jitter corresponding to 20% of the stimulus radius. The overall presentation of each stimulus was Gaussian contrast enveloped in time with a sigma of 125 ms centered on the temporal window and the stimuli appeared within a temporal interval of 1 s. Auditory feedback was given after each trial. A black fixation mark was presented in the centre of the display and subjects were asked to maintain their

Table 1

The combinations of spatial frequency and radii tested in Figs. 2A and 2B are indicated by a check. Crosses indicate combinations that could not be tested due to stimulus resolution limitations. In Fig. 3 an additional combination of SF = 2 cpd and R = 2.5° was tested.

Spatial frequency (cpd)	Radius (°)				
	0.5	1	2.5	5.5	10.5
10	✓	✓	×	×	×
5	✓	✓	✓	×	×
1	×	×	✓	✓	✓

fixation during the whole presentation. Practice trials were run before the experiments commenced. All experiments were done under binocular viewing conditions. In Section 3 we plot shape discrimination threshold as a percent change of the radial amplitude modulation (RAM) rather than absolute units. This is used since a constant % RAM reflects constant shape proportions and so is the relevant metric for investigating shape constancy.

2.4. Observers

Six experienced psychophysical observers participated in this study, two of whom were the authors, while the others were naïve

with regard to the aims of the experiments. All have normal, or corrected to normal vision, and all have normal color vision according to the Farnsworth-Munsell 100-Hue Test.

3. Results

3.1. RF contour spatial frequency and scaling effects

In this experiment we investigate whether the contour spatial frequency and the size (radius) of the stimuli affect shape discrimination thresholds for RF patterns matched for visibility in multiples of detection threshold. We varied independently the contour spatial frequency and the pattern radius (see Fig. 1C and B) for radial frequency patterns over the range from 2 (oval) to 6 (hexagon). We examined a range of radii (0.5°, 1°, 2° and 2.5°) and contour spatial frequencies (1, 2.5, 5 and 10 cpd), as detailed in Table 1. Some combinations could not be obtained due to stimulus resolution limitations. Results are shown in Fig. 2A for one observer and the average of three observers in Fig. 2B. For all observers, there was significant effect of varying the contour spatial frequency while the radius was fixed (left columns in Figs. 2A and 2B). Data for all observers were consistent and in the range 1–10 cpd average thresholds for the higher spatial frequency are better than for the lower spatial frequency at each fixed radius. Figs. 2A and 2B (right

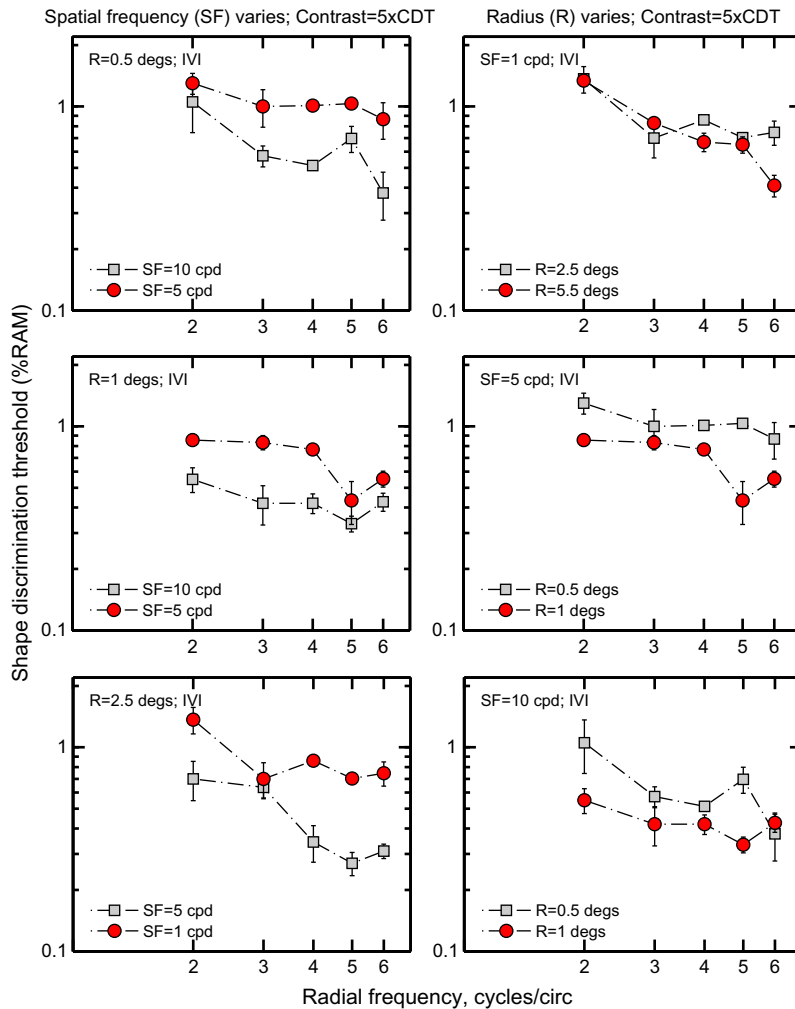


Fig. 2A. Shape discrimination thresholds for RF patterns (% RAM) plotted as function of radial frequency (in cycles/circ). Results are shown for one observer (IVI). The spatial frequency (SF) of the pattern is 10 cpd, 5 cpd or 1 cpd, while the radius is 0.5°, 1° or 2.5°. The left column shows the condition in which the radius is fixed at 0.5°, 1° or 2.5° and the SF varies, while the right column shows the condition in which SF is fixed at 1, 5 or 10 cpd and the radius varies. Error bars are ±1 standard error of the mean (SEM).

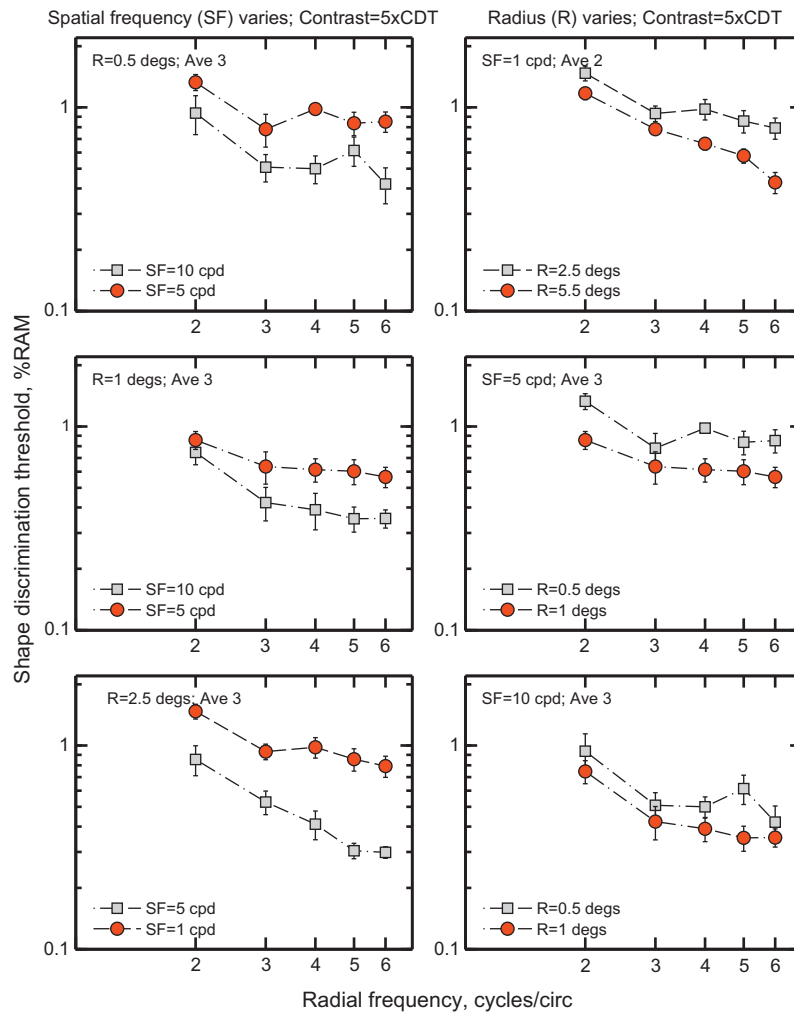


Fig. 2B. As for Fig. 2A but average results (Ave) for all observers tested, as indicated in each panel.

columns) show the condition where spatial frequency is fixed and the radius is varied. It is clear that there is significant improvement of performance (lower thresholds) for the longer stimulus radii at each contour spatial frequency. These results indicate that, over the range investigated, the shape discrimination thresholds are dependent both on the contour spatial frequency and on the size (radius) of the patterns.

We next investigated directly whether shape discrimination thresholds are robust to changes in viewing distance (Fig. 1D). Fig. 3 shows individual and group results when the relationship between spatial frequency and size is varied inversely, as when viewing distance is varied. Shape discrimination thresholds are plotted as function of the radial frequency investigated. Data are for the individual observers and the average of the group. To test for significant difference in the group data we used a one-way ANOVA, post hoc corrected with Tukey's honesty criterion. For each condition (RF2, RF3, RF4, RF5 and RF6) an ANOVA with a factor of stimulus features ($R = 0.5^\circ$ and $SF = 10$ cpd vs. $R = 1^\circ$ and $SF = 5$ cpd vs. $R = 2.5^\circ$ and $SF = 2$ cpd) was used to test for any main effects. The average shape discrimination thresholds, for the three different radii and spatial frequency combinations tested ($R = 0.5^\circ$ and $SF = 10$ cpd; $R = 1^\circ$ and $SF = 5$; $R = 2.5^\circ$ and $SF = 2$ cpd) were not significantly different for the conditions tested (RF2: $F(2,8) = 0.76$, $p = 0.5$; RF3: $F(2,8) = 3.07$, $p = 0.12$; RF4: $F(2,8) = 1.6$, $p = 0.27$; RF5: $F(2,8) = 0.7$, $p = 0.53$; RF6: $F(2,8) = 4.3$, $p = 0.07$). The results are consistent with the data in Figs. 2A and 2B in which it was ob-

served that an increase of pattern spatial frequency or radius results in lower shape discrimination thresholds. These results as well as the results in Figs. 2 indicate that, over the ranges investigated, the shape discrimination thresholds are dependent on the spatial frequency as well as on the size of the pattern. Distance scaling is obtained as the effects of spatial frequency and radius on threshold vary in inverse proportion.

For two observers, we further expanded the parameter space and investigated a larger range of radial frequencies (2–32 cycles/circ) and radii (2.5–10.5 $^\circ$), while the contour spatial frequency was fixed at 1 cpd. Results are presented in Fig. 4. Shape discrimination thresholds in percent radial amplitude modulation are plotted as function of radial frequency (Fig. 4). It is evident that at all pattern radial frequencies investigated there was an improvement in performance (lower thresholds) with increasing radius. Thus, these results (Figs. 2A–4) differ from those of Wilkinson, Wilson, and Habak (1998), who demonstrated invariance of thresholds over a similar range of spatial frequency and radius that we investigated in Figs. 2.

3.2. RF contour contrast effect

One of the key differences between our experiments and those of Wilkinson, Wilson, and Habak (1998) is the contrast of the stimuli used. In our study, stimuli are presented at five times detection threshold, whereas Wilkinson, Wilson, and Habak (1998) presented stimuli at a fixed 100% contrast. This suggests that there

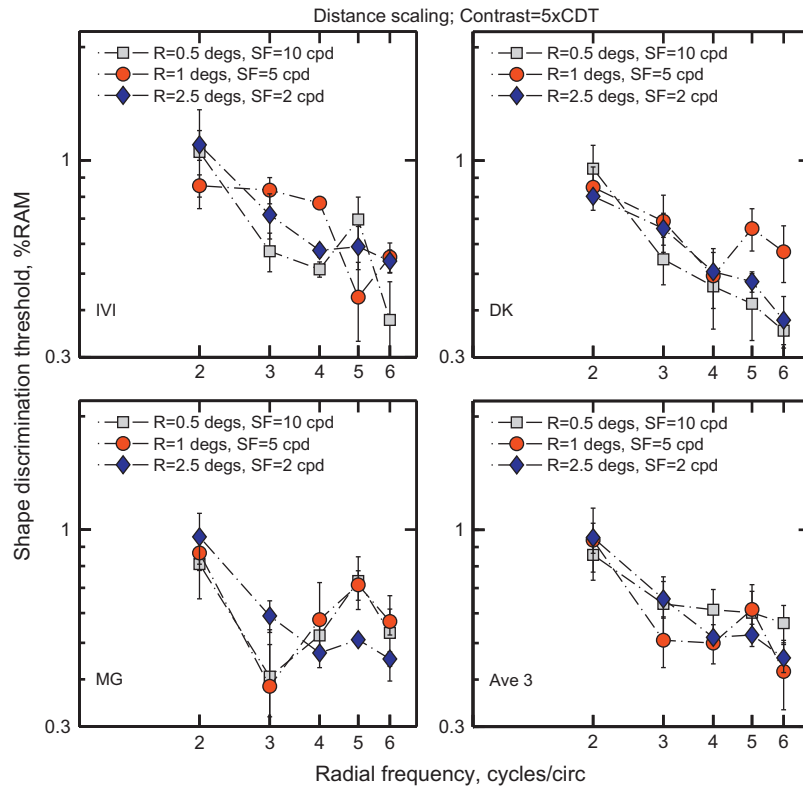


Fig. 3. Shape discrimination thresholds for RF patterns (in % RAM) plotted as function of radial frequencies (in cycles/circ); radius (R) and spatial frequency (SF) are varied inversely as when viewing distance is varied. Lower right panel shows individual results for the group data. Gray squares are for patterns with $R = 0.5$ and $SF = 10$ cpd. Red circles represent patterns with $R = 1$ and $SF = 5$ cpd, which correspond to a decrease of the viewing distance by a factor of 2. Error bars are ± 1 SEM. (For interpretation of the references to color in this figure legend, the reader is referred to the web version of this article.)

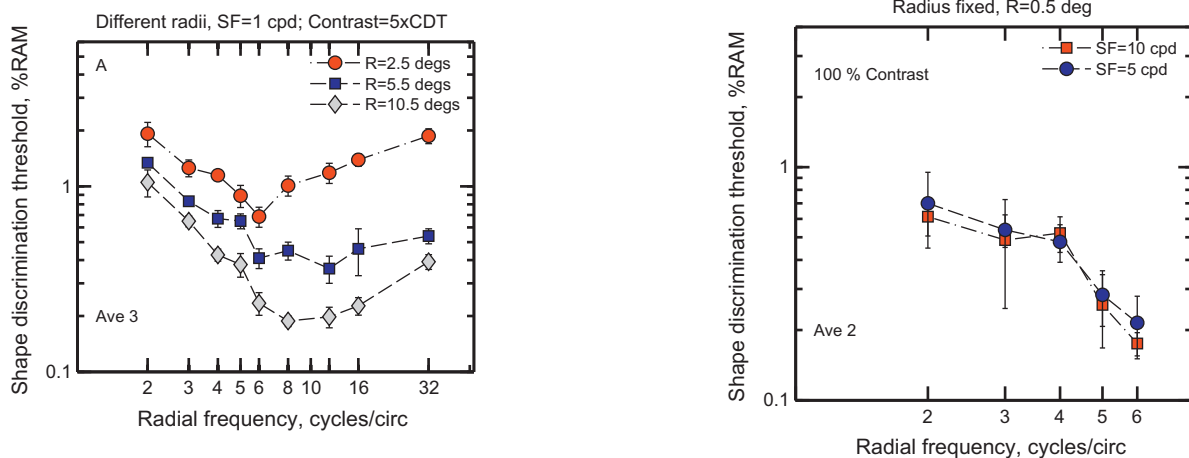


Fig. 4. Average shape discrimination thresholds for RF patterns (in % RAM) plotted as function of pattern radial frequency (in cycles/circ) for three observers. Different colors represent different radii: red circles for $R = 2.5^\circ$; blue squares for $R = 5.5^\circ$; gray diamonds for $R = 10.5^\circ$. Error bars are ± 1 SEM. (For interpretation of the references to color in this figure legend, the reader is referred to the web version of this article.)

Fig. 5. Shape discrimination thresholds for RF patterns (in % RAM) are plotted as function of radial frequency (in cycles/circ). Mean results for two observers. The spatial frequency (SF) of the pattern is 10 cpd (red squares) or 5 cpd (blue circles), while the radius is set to 0.5° . Stimuli are presented at 100% contrast. Error bars are ± 1 SEM. (For interpretation of the references to color in this figure legend, the reader is referred to the web version of this article.)

may be an important role of contrast in shape discrimination. To investigate this we first repeated one of the conditions in the original study using high contrast stimuli in order to verify the results of Wilkinson, Wilson, and Habak (1998) for our experimental set-up. Results from this control experiment are shown in Fig. 5, in which we fix the radius of the RF pattern at 5° and vary the spatial frequency (5 cpd and 10 cpd). The data are the average across two subjects and show no significant effect of the spatial frequency on

the shape discrimination thresholds, replicating the results of Wilkinson, Wilson, and Habak (1998). These data confirm that differences between our data and the earlier study of Wilkinson, Wilson, and Habak (1998) are genuine and may reflect the important role of stimulus contrast in shape discrimination tasks.

In Fig. 6 we investigate the effect of contrast on discrimination thresholds for spatial frequencies 1 cpd and 5 cpd at a smaller fixed size ($R = 2.5^\circ$) and for spatial frequencies 5 cpd and 10 cpd at a

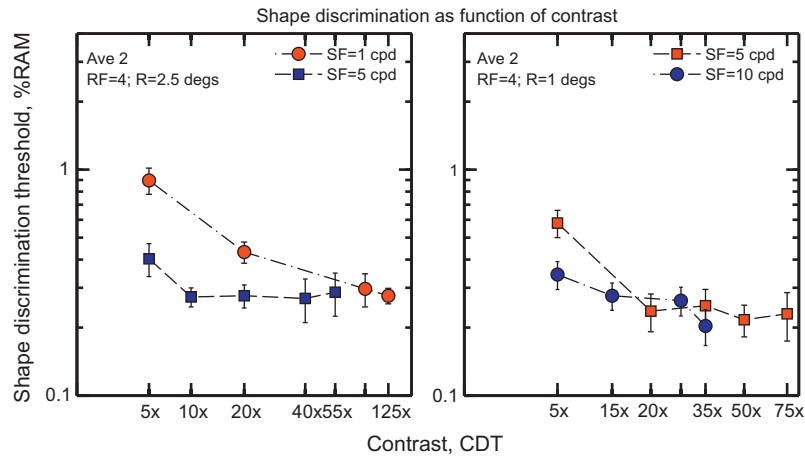


Fig. 6. Shape discrimination thresholds plotted as function of contrast for RF4 patterns at fixed radius ($R = 2.5^\circ$, left plot, or $R = 1^\circ$, right plot). Results for spatial frequencies (SF) of 1 cpd (in red circles) and 5 cpd (in blue squares) at $R = 2.5^\circ$ on the left plot, and 5 cpd (in red squares) and 10 cpd (in blue circles) at $R = 1^\circ$ on the right plot are shown. Group data are plotted. The stimuli were scaled in multiples of contrast detection threshold (CDT), plotted on the x-axis. On the left plot, at $R = 2.5^\circ$ 100% contrast was reached at $55 \times$ CDT for SF = 5 cpd and at $125 \times$ CDT for SF = 1 cpd. On the right plot, at $R = 1^\circ$ on average 100% contrast was reached at $35 \times$ CDT for SF = 10 cpd and at $75 \times$ CDT for SF = 5 cpd. Error bars are ± 1 SEM. (For interpretation of the references to color in this figure legend, the reader is referred to the web version of this article.)

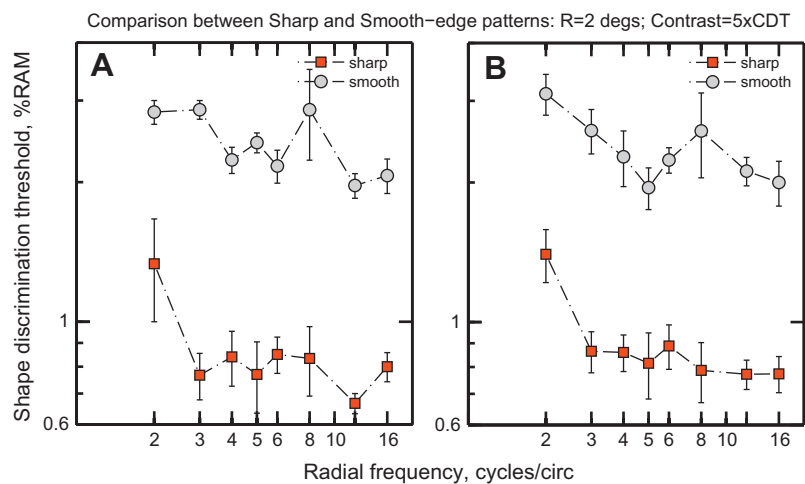


Fig. 7. Shape discrimination thresholds (in % RAM) plotted as function of different radial frequencies (in cycles/circ) for the surface-RF patterns. Figure (A) and (B) show individual and averaged data, respectively, for the comparison sharp vs. smooth-edge conditions. Red squares are for the sharp edge condition, while the gray circles are for the smooth edge condition (SF = 1 cpd). Error bars are ± 1 SEM. (For interpretation of the references to color in this figure legend, the reader is referred to the web version of this article.)

smaller fixed size ($R = 1^\circ$) for a fixed radial frequency (RF = 4). In the left plot, stimuli were presented at contrasts from $5 \times$ to $55 \times$ contrast detection threshold (CDT) for a contour SF of 5 cpd ($55 \times$ CDT = 100% contrast) and from $5 \times$ to $125 \times$ CDT for SF = 1 cpd ($125 \times$ CDT = 100% contrast), both at $R = 2.5^\circ$. In the right plot, for $R = 1^\circ$, stimuli were presented at contrasts from $5 \times$ to $35 \times$ CDT for a contour SF = 10 cpd ($35 \times$ CDT = 100% contrast, on average) and from $5 \times$ to $75 \times$ CDT for SF = 5 cpd ($75 \times$ CDT = 100% contrast, on average). It is evident that shape discrimination thresholds vary differentially with contrast and are significantly different at lower contrasts, while at the higher contrasts the difference is not significant. The data from this experiment are consistent with earlier data from Mullen and Beaudot (2002) showing that shape discrimination improves with contrast and suggest an important role of contrast in shape discrimination tasks. We conclude that the reason Wilkinson, Wilson, and Habak (1998) found that contour spatial frequency and radius have no effect on shape discrimination was due to the high stimulus contrasts used.

3.3. Surface-RF pattern discrimination for sharp (high spatial frequency) vs. smooth (low spatial frequency) edges

In this experiment we compared shape discrimination for surface-RF patterns with high and low spatial frequency edges. We argue that an effect of spatial frequency on shape discrimination threshold for these patterns would suggest that a similar mechanism is processing contour and surface defined RF patterns. Results from this experiment are shown in Fig. 7 for the two different stimulus conditions (sharp- and smooth-edged) for the four subjects that took part in this experiment. Fig. 7A shows individual data for a typical observer (IV), for the sharp- and smooth-edged conditions. Data for the other observers are similar, and the average of all are shown in Fig. 7B. Shape discrimination thresholds are plotted as function of the different radial frequencies tested (2–16 cycles/circ) at fixed radius of 2° . Shape discrimination thresholds for the smooth condition are on average $2.5 \times$ higher than the thresholds for the sharp condition and are significantly

different. The very steep decline in thresholds in the smooth condition (Fig. 7A and B, circles) demonstrates an improvement of shape discrimination performance with the increase of the radial frequency from 2 to 5, which is similar to results reported previously for RF contour patterns (Mullen & Beaudot, 2002; Mullen, Beaudot, & Ivanov, 2011). This steep decline in shape discrimination with increasing pattern frequency has been attributed to the local orientation variations in the contour (Mullen, Beaudot, & Ivanov, 2011). In Fig. 7A and B (squares) individual data of a typical observer and the average of the group are shown, respectively, in the sharp surface-RF pattern condition. It is evident that for radial frequencies above 3 cycles/circ. shape discrimination thresholds are constant in contrast with the steep decline in thresholds for the smooth condition. This type of performance, for RF patterns, has been reported by Wilkinson, Wilson, and Habak (1998) and argued to indicate the global processing nature of shape discrimination at threshold. Thus, our results that discrimination thresholds are constant for radial frequencies above 3 cycles/circ in the high frequency condition and the decline in thresholds for radial frequency from 2 to 5 in the low spatial frequencies condition are compatible with those for the contour-SF condition in Fig. 2B.

4. Discussion

The purpose of this study was to resolve the controversy over whether the shape discrimination of RF patterns is invariant with the local cue changes of pattern radius and contour spatial frequency, as proposed by Wilkinson, Wilson, and Habak (1998) and supported by the data of Achtman, Hess, and Wang (2003), and to investigate the effect of contrast on this. As reviewed in the Introduction, the previous literature on this issue has been conflicting and unresolved, with some studies finding that shape discrimination is invariant with pattern size (radius), contour spatial frequency, and contrast (Achtman, Hess, & Wang, 2003; Wilkinson, Wilson, & Habak, 1998), while others have shown a dependence on these features (Mullen & Beaudot, 2002; Mullen, Beaudot, & Ivanov, 2011). At issue is the question of the stage in the shape processing hierarchy at which shape discrimination thresholds are limited. Wilkinson, Wilson, and Habak (1998) found that the RF patterns at threshold always had the same proportions, since radial modulation at threshold was always a constant % of the radius, despite differences in spatial frequency, radius, and overall pattern shape (radial frequency). They argued that this was consistent with threshold reflecting a global processing stage that had achieved shape constancy, a result which was backed-up by other lines of evidence presented in support of global processing. On the other hand, Mullen, Beaudot, and Ivanov (2011) using low contrast stimuli argued that shape discrimination thresholds are limited by the ability to detect local variations in orientation or curvature of the contour, and demonstrated that the influence of the parameters of stimulus size (radius) and radial frequency on shape discrimination could be understood in terms of their effect on local orientation and curvature cues. Global pooling mechanisms, however, may fail at low contrasts allowing non-global mechanism to limit shape discrimination. Thus in order to understand the nature of the differences among the studies and resolve these issues, we used an extensive range of parameters to cover those used in previous studies, which have typically used different ranges of spatial frequency and radii (Wilkinson, Wilson, & Habak, 1998; Mullen & Beaudot, 2002; Mullen, Beaudot, & Ivanov, 2011). We have also investigated the role of contrast, which we show to be key to the issue.

The range of spatial frequencies and radii we use in this paper (1–10 cpd, 0.5–10°) includes most of the combined ranges used by both Wilkinson, Wilson, and Habak (1998) (4–16 cpd, 0.25–1°)

and Mullen, Beaudot, and Ivanov (2011) (0.75–6 cpd, 0.3–2.4°), with the exception of the extreme values at either ends of the range. Our results (Figs. 2–4) demonstrate a clear effect on shape discrimination thresholds of spatial frequency at a fixed radius, with threshold improvements found for contours with higher spatial frequencies. Threshold improvements were also found for shapes with larger radii at a fixed spatial frequency, consistent with effects reported previously (Mullen & Beaudot, 2002; Mullen, Beaudot, & Ivanov, 2011). Across the data in Figs. 2–5 there is also an effect of radial frequency on shape discrimination threshold, with improvements in threshold for RF shapes from 2 to 4 cycles (ovals–squares) and optimal thresholds for shapes with 4 to 6 cycles (squares–hexagons), also consistent with previous results (Mullen & Beaudot, 2002; Mullen, Beaudot, & Ivanov, 2011). Thus these results, in general, argue against the existence of shape constancy at threshold.

A more specific effect, that of distance scaling, was confirmed by the data (Fig. 3). If contour spatial frequency and radius are varied in inverse proportion, as occurs when viewing distance is changed, shape discrimination thresholds remain constant. We show this effect holds across different RF shapes from 2 to 6 cycles/circ. In other words, we find that thresholds are constant in terms of shape proportion (% RAM) as long as the ratio of contour thickness (1/SF) to radius is fixed. This effect has been reported previously for two different ratios of contour thickness to radius, one similar to the one we used here (Wilkinson, Wilson, & Habak, 1998) and one very different (Mullen, Beaudot, & Ivanov, 2011), and hence this effect appears to be quite general. It is important to note, however, that this effect is not part of a more general principle of shape constancy, as we discounted above.

The clear improvements in shape discrimination we find with increasing contour spatial frequency and increasing shape size (radius) clearly differ from the results reported by Wilkinson, Wilson, and Habak (1998), who found invariance with these parameters. The source of the differences appears to be the stimulus contrast used; we use a relatively low contrast of five times detection threshold, whereas Wilkinson, Wilson, and Habak (1998) used a fixed contrast of the maximum value (100%). We first replicated their results for our stimuli presented at 100% contrast (Fig. 5), so discounting any other differences between the two experiments. We then demonstrated that contrast has a differential effect on shape discrimination thresholds depending on the spatial frequency of the contour (Fig. 6). We find an exponential improvement in threshold as a function of contrast, reaching an asymptote at high contrasts, as previously reported using different stimulus parameters (Mullen & Beaudot, 2002). These differences remain even when stimuli are scaled in units of % contrast. At a contrast of approximately 55× detection threshold, shape discrimination thresholds for both the larger patterns tested (1 and 5 cpd; 2.5°, Fig. 4A) had asymptoted to the same threshold value. Similar asymptotic behavior was observed for the smaller patterns tested (5 and 10 cpd; 1°, Fig. 4B, with asymptotic value reached at 20× detection threshold). At contrasts below this, there was a steeper loss of shape discrimination thresholds for the lower spatial frequency. Thus at very high contrasts, the differential effects of pattern radius and contour spatial frequency, which are apparent at lower contrasts, disappear. Our results suggest that interactions among stimulus contrast, contour spatial frequency and radius can influence shape discrimination and are indicative of the role of local shape cues in determining threshold. Similar effects may also account for the invariance with spatial frequency found in other shape discrimination studies (Achtman, Hess, & Wang, 2003).

The significant influence of contrast, contour spatial frequency and radius on shape discrimination thresholds suggests that local cues may limit shape discrimination at threshold. Mullen, Beaudot, and Ivanov (2011) have shown that the shape discrimination

threshold for a single cycle of an RF pattern presented alone is as good as for the whole pattern, indicating that information within a single cycle is sufficient to support threshold and arguing against an influence of global processing. Stimulus presentations using less than a single cycle produced a sharp deterioration in threshold, suggesting that optimal thresholds require the integration of information across one whole RF cycle. Thus, although not global in the sense of requiring pooling of information across the whole RF shape, the requirement of a single cycle for shape discrimination is also not strictly local in the sense that it cannot be computed by single, orientation-tuned neurons in V1. Instead, discrimination based on a single RF cycle requires the estimation of the pattern origin and the appropriate orientation or curvature computations along the pattern cycle, and so is likely to engage an intermediate stage of contour processing of the type that might be found in V2 or V4 (Pasupathy, 2006; Pasupathy & Connor, 1999). Mullen, Beaudot, and Ivanov (2011) used a model that calculated the orientation variation in one RF cycle to predict the improvement in threshold found as RF shape (radial frequency) increased from 2 to 6 cycles, however, other quasi-local cues such as curvature may also be used.

The use of quasi-local cues such as orientation variation and curvature to determine threshold provides a basis for understanding the influence of stimulus parameters such as contrast, contour spatial frequency and radius. Contrast is known to influence orientation discrimination, with performance improving with contrast until asymptotic performance levels are reached, typically by about 10% contrast, but depending on the stimulus area (Mareschal & Shapley, 2004; Webster, De Valois, & Switkes, 1990). This effect is probably mediated through the effect of contrast on the receptive field properties of V1 neurons (Angelucci et al., 2002; Kapadia, Westheimer, & Gilbert, 1999; Sceniak et al., 1999). Orientation discrimination also depends on stimulus spatial frequency with performance deteriorating at lower spatial frequencies below 1 cpd (Burr & Wijesundra, 1991), an effect which is also contrast dependent. Thus the interactions between contrast, spatial frequency and stimulus area are complex, even for simple grating stimuli, but in general predict better orientation discrimination for higher contrasts and higher spatial frequencies. Our shape discrimination thresholds show a similar broad dependence on contrast and spatial frequency, supporting the importance of quasi-local cues at shape discrimination threshold. The saturation of orientation discrimination at high contrasts may account for why shape discrimination thresholds asymptote at high contrasts. The deterioration in orientation discrimination at low spatial frequencies may also contribute to the deterioration of shape discrimination thresholds for thicker contours below 1 cpd. This effect will also be influenced, however, by the increase in the orientation bandwidth of the stimuli at lower spatial frequencies, which depends on the aspect ratio of the local contour, since broader orientation bandwidths are associated with reduced orientation discrimination (Beaudot & Mullen, 2005, 2006). It is interesting that distance scaling preserves the aspect ratios of the stimuli, and also preserves shape discrimination thresholds.

We have also shown that increasing stimulus size (radius) improves shape discrimination thresholds, and it is surprising that this effect continues even up to extremely large stimuli with radii of 10.5° . In fact, some of the best thresholds we obtained were for the largest pattern used (10.5°). We note that this improvement is in shape discrimination thresholds expressed as a proportion of the radius (% RAM) (Fig. 4), showing that shape proportion is not maintained at threshold with increasing radius but becomes closer to the perfect circle. This effect is not what would be expected from a global process that has shape constancy, and suggests that other factors are influencing threshold. For example, curvature decreases with increasing radius, and Watt and Andrews (1982) have found

that curvature discrimination (for curved lines of fixed length) is better for lower compared to higher curvatures, suggesting that local curvature discriminations may be better for larger RF patterns with lower curvatures than for smaller patterns with higher curvatures.

We also tested some of our results on filled patterns (Fig. 7), chosen because they are very similar to stimuli that activate single neurons in primate V4 (Pasupathy, 2006; Pasupathy & Connor, 1999, 2002). The results generally support our findings for the contour-based RF patterns. There is a clear effect of edge properties on shape discrimination thresholds. Stimuli with sharp edges, containing high spatial frequencies, are much better discriminated (by about 4-fold) than those with smoothed edges containing only lower spatial frequencies. This is similar to the spatial frequency effects found for the RF patterns in Figs. 2A and 2B. Thresholds for the sharp-edged filled patterns were similar to the thresholds of the contour based patterns (at equivalent radii), generally supporting the idea that similar mechanisms are processing both contour- and surface-defined RF patterns. The sharp edged stimuli appear to have a flatter dependence on radial frequency than the smoothed-edge ones, resembling the data of Figs. 2A and 2B, although this would have to be confirmed on more subjects.

Wilkinson, Wilson, and Habak (1998) and Achtman, Hess, and Wang (2003) argue that because performance remains invariant with local cue changes (such as radius, spatial frequency and contrast among others) shape discrimination thresholds are limited by global pooling. In our experiments shape discrimination is clearly *not* invariant with the systematic manipulation of a series of single local features such as spatial frequency and size at relatively low contrasts. At higher contrasts (10–20 \times threshold) there is, however, much less dependence on spatial frequency and radius. This suggests that non-global processing is involved at low contrasts, whereas performance may still be limited by global processing at higher contrasts.

5. Conclusions

We show that shape discrimination thresholds for RF patterns have a complex series of dependencies on the stimulus size (radius), contour spatial frequency (thickness) and contrast. Because these dependencies saturate at high contrasts, these relationships were not found in previous studies that used high stimulus contrasts. We conclude that there is no evidence for shape constancy at shape discrimination thresholds for radial frequency patterns, although distance scaling of threshold for stimuli of fixed proportions is found. We show that discrepancies between earlier studies can be accounted for by a differential effect of contrast on shape discrimination, with shape invariance only stabilizing at higher contrasts (10–20 \times threshold). Our interpretation of the lost shape constancy at low contrast is that shape discrimination may be limited by non-global processing.

Acknowledgments

This study was funded by a CIHR Grant to K.T. Mullen (MOP-10819). The authors thank Daniel Kramer, Luis Garcia Suarez, Mina Gheiratmand and Niia Nikolova for their help in collecting data. We thank the two anonymous reviewers for their useful comments.

References

- Achtman, R. L., Hess, R. F., & Wang, Y. (2003). Sensitivity for global shape detection. *Journal of Vision*, 3, 616–624.
- Angelucci, A., Levitt, J. B., Walton, E. J. S., Hupe, J., Bullier, J., & Lund, J. S. (2002). Circuits for local and global signal integration in primary visual cortex. *Journal of Neuroscience*, 22, 8633–8646.

- Beaudot, W. H., & Mullen, K. T. (2005). Orientation selectivity in luminance and color vision assessed using 2-d band-pass filtered spatial noise. *Vision Research*, 45, 687–696.
- Beaudot, W. H., & Mullen, K. T. (2006). Orientation discrimination in human vision: Psychophysics and modeling. *Vision Research*, 46, 26–46.
- Bell, J., Badcock, D. R., Wilson, H., & Wilkinson, F. (2007). Detection of shape in radial frequency contours: Independence of local and global form information. *Vision Research*, 47, 1518–1522.
- Burr, D. C., & Wijesundra, S. A. (1991). Orientation discrimination depends on spatial frequency. *Vision Research*, 31, 1449–1452.
- Dobbins, A., Zucker, S. W., & Cynader, M. S. (1987). Endstopped neurons in the visual cortex as a substrate for calculating curvature. *Nature*, 329, 438–441.
- Dobbins, A., Zucker, S. W., & Cynader, M. S. (1989). Endstopping and curvature. *Vision Research*, 29, 1371–1387.
- Dumoulin, S. O., & Hess, R. F. (2007). Cortical specialization for concentric shape processing. *Vision Research*, 47, 1608–1613.
- Fujita, I., Tanaka, K., Ito, M., & Cheng, K. (1992). Columns for visual features of objects in monkey inferotemporal cortex. *Nature*, 360, 343–346.
- Gallant, J. L., Braun, J., & Van Essen, D. C. (1993). Selectivity for polar, hyperbolic, and Cartesian gratings in macaque visual cortex. *Science*, 259, 100–103.
- Gallant, J. L., Shoup, R. E., & Mazer, J. A. (2000). A human extrastriate area functionally homologous to macaque v4. *Neuron*, 27, 227–235.
- Gross, C. G., Rocha-Miranda, C. E., & Bender, D. B. (1972). Visual properties of neurons in inferotemporal cortex of the macaque. *Journal of Neurophysiology*, 35, 96–111.
- Hess, R. F., Wang, Y., & Dakin, S. C. (1999). Are judgements of circularity local or global? *Vision Research*, 39, 4354–4360.
- Hess, R. F., Wang, Y.-Z., Demanins, R., Wilkinson, F., & Wilson, H. R. (1999). A deficit in strabismic amblyopia for global shape detection. *Vision Research*, 39, 901–914.
- Hubel, D. H., & Wiesel, T. N. (1968). Receptive fields and functional architecture of monkey striate cortex. *The Journal of Physiology (London)*, 195, 215–243.
- Ito, M., Tamura, H., Fujita, I., & Tanaka, K. (1995). Size and position invariance of neuronal responses in monkey inferotemporal cortex. *Journal of Neurophysiology*, 73, 218–226.
- Jeffrey, B. G., Wang, Y. Z., & Birch, E. E. (2002). Circular contour frequency in shape discrimination. *Vision Research*, 42, 2773–2779.
- Kapadia, M. K., Westheimer, G., & Gilbert, C. D. (1999). Dynamics of spatial summation in primary visual cortex of alert monkeys. *Proceedings of the National Academy of Sciences of the United States of America*, 96, 12073–12078.
- Loffler, G. (2008). Perception of contours and shapes: Low and intermediate stage mechanisms. *Vision Research*, 48, 2106–2127.
- Loffler, G., Wilson, H. R., & Wilkinson, F. (2003). Local and global contributions to shape discrimination. *Vision Research*, 43, 519–530.
- Logothetis, N. K., Pauls, J., & Poggio, T. (1995). Shape representation in the inferior temporal cortex of monkeys. *Current Biology*, 5, 552–563.
- Mareschal, I., & Shapley, R. M. (2004). Effects of contrast and size on orientation discrimination. *Vision Research*, 44, 57–67.
- Mullen, K. T., & Beaudot, W. H. (2002). Comparison of color and luminance vision on a global shape discrimination task. *Vision Research*, 42, 565–575.
- Mullen, K. T., Beaudot, W. H. A., & Ivanov, I. V. (2011). Evidence that global processing does not limit thresholds for RF shape discrimination. *Journal of Vision*, 11(3), 1–21. 6.
- Pasupathy, A. (2006). Neural basis of shape representation in the primate brain. *Progress in Brain Research*, 154, 293–313.
- Pasupathy, A., & Connor, C. E. (1999). Responses to contour features in macaque area v4. *Journal of Neurophysiology*, 82, 2490–2502.
- Pasupathy, A., & Connor, C. E. (2001). Shape representation in area v4: Position-specific tuning for boundary conformation. *Journal of Neurophysiology*, 86, 2505–2519.
- Pasupathy, A., & Connor, C. E. (2002). Population coding of shape in area v4. *Nature Neuroscience*, 5, 1332–1338.
- Poirier, F. J. A. M., & Wilson, H. R. (2007). Object perception and masking: Contributions of sides and convexities. *Vision Research*, 47, 3001–3011.
- Reddy, L., & Kanwisher, N. (2006). Coding of visual objects in the ventral stream. *Current Opinion in Neurobiology*, 16, 408–414.
- Sceniak, M. P., Ringach, D. L., Hawken, M. J., & Shapley, R. (1999). Contrast's effect on spatial summation by macaque v1 neurons. *Nature Neuroscience*, 2, 733–739.
- Wang, Y., & Hess, R. F. (2005). Contributions of local orientation and position features to shape integration. *Vision Research*, 45, 1375–1383.
- Wang, Y.-Z., Wilson, E., Locke, K., & Edwards, A. O. (2002). Shape discrimination in age-related macular degeneration. *Investigative Ophthalmology and Visual Science*, 43, 2055–2062.
- Watt, R. J., & Andrews, D. P. (1982). Contour curvature analysis: Hyperacuties in the discrimination of detailed shape. *Vision Research*, 22, 449–460.
- Webster, M. A., De Valois, K. K., & Switkes, E. (1990). Orientation and spatial-frequency discrimination for luminance and chromatic gratings. *Journal of the Optical Society of America A*, 7, 1034–1049.
- Wilkinson, F., James, T. W., Wilson, H. R., Gati, J. S., Menon, R. S., & Goodale, M. A. (2000). An fMRI study of the selective activation of human extrastriate form vision areas by radial and concentric gratings. *Current Biology*, 10, 1455–1458.
- Wilkinson, F., Wilson, H. R., & Habak, C. (1998). Detection and recognition of radial frequency patterns. *Vision Research*, 38, 3555–3568.
- Wilson, H. R. (1999). Non-fourier cortical processing in texture, form, and motion. In P. S. U. E. G. Jones (Ed.), *Cerebral cortex: Models of cortical circuitry* (pp. 445–477). New York: Kluwer Academic/Plenum Publishers.
- Wilson, H. R., & Wilkinson, F. (1997). Evolving concepts of spatial channels in vision: From independence to nonlinear interactions. *Perception*, 26, 939–960.